Optics & Laser Technology 91 (2017) 166–174

Contents lists available at ScienceDirect

Optics & Laser Technology

journal homepage: www.elsevier.com/locate/optlastec

Full length article

Preparation and characterization silver/zirconium nickel oxide nanocomposites with negative electromagnetic parameters

Reza Gholipur*, Ali Bahari

Department of Solid State Physics, University of Mazandaran, Mazandaran, Babolsar 4741695447, Iran

ARTICLE INFO

Keywords:
Nanostructure
Magnetic properties
Electrical properties

ABSTRACT

Different amounts of silver (0–45 wt%) have been synthesized with $Zr_{0.9}Ni_{0.1}O_y$ based on co-precipitation technique. Doping with silver metal is an interesting way to achieve the double negative (DNG) properties. The morphology and structure properties of $Ag/Zr_{0.9}Ni_{0.1}O_y$ nanocomposite were studied by x-ray diffraction (XRD), scanning electron microscopy (SEM) and transmission electron microscopy (TEM) techniques. The XRD analysis showed that no reaction took place between $Zr_{0.9}Ni_{0.1}O_y$ and silver during calcination and sintering. SEM observation showed that the silver particles presented homogenous particle distribution in the $Zr_{0.9}Ni_{0.1}O_y$ matrix. The electrical and magnetic properties of the silver-doped $Zr_{0.9}Ni_{0.1}O_y$ were investigated. It was found that silver doping results in both negative permittivity and negative permeability possibly due to the incorporation of Ag atoms in the percolation network. Our results suggest that the $Ag/Zr_{0.9}Ni_{0.1}O_y$ is a suitable candidate for DNG materials.

1. Introduction

Recently the metamaterials of the single negative (SNG), or DNG, which simultaneously possess negative permittivity and negative permeability, attract much attention due to several possible applications such as perfect lens, microwave absorbers, antenna radomes [1–13], reverse Vavilov-Cherenkov effect [14], negative refraction [15], cloaking [16–19], concentrator [20], and negative compressibility [21]. So far, many research works have been conducted on understanding the physical properties and on realization or synthesis of DNG metamaterials [22–31].

These materials derive their unique properties from the collective response of ordered [32–37] or disordered subwavelength resonant cells [38]. That is to say, the negative permittivity and permeability of metamaterials originate from artificial structures rather than directly from the materials' intrinsic properties.

In recent years, researchers have begun to search for the materials with inherent DNG property. However, there are few research works that have been reported to realize negative permittivity [39–41] or negative permeability [42,43] using the materials' intrinsic properties. Metal-dielectric nanocomposites have great potential in the preparation of single or double negative materials, as has been shown by Ao et al. [44,45].

In the present work, Ag networks were hosted in $Zr_{0.9}Ni_{0.1}O_y$ medium through co-precipitation technique which includes two steps: $Zr_{0.9}Ni_{0.1}O_y$ synthesis, and silver nanoparticles growth. The main text of this paper includes the following parts: In the composition, microstructure, and electromagnetic properties of the $Ag/Zr_{0.9}Ni_{0.1}O_y$ nanocomposite are discussed. Interestingly, negative permittivity and negative permeability appeared in the composites with Ag content of 45 wt%. For the sample with Ag content of 45 wt%, negative permittivity and negative permeability were obtained at similar frequency region.

2. Experimental

2.1. $Zr_{0.9}Ni_{0.1}O_y$ synthesis

The $Zr_{0.9}Ni_{0.1}O_y$ was prepared using co-precipitation technique. The Starting precursors were Zirconyl chloride octahydrate [$ZrOCl_2 \cdot 8H_2O$] and nickel(II) chloride [$NiCl_2 \cdot 6H_2O$]. The Zr/Ni solution was prepared by dissolving Zirconyl chloride octahydrate and nickel(II) chloride in double distilled water. The molar ratio of the Zr and Ni was according to Zr/Ni =9. Ammonia solution was then added directly to the Zr/Ni solution drop-by-drop while stirring.

2.2. Silver nanoparticles growth

Silver nitrate [AgNO3], n,n-dimethylformamide (DMF) [C_3H_7ON], Polyvinyl pyrrolidone (PVP) and chloroauric acid ($HAuCl_4$) were used

* Corresponding author.
E-mail address: gholipur.reza@gmail.com (R. Gholipur).

http://dx.doi.org/10.1016/j.optlastec.2016.12.034
Received 14 July 2016; Received in revised form 25 November 2016; Accepted 27 December 2016

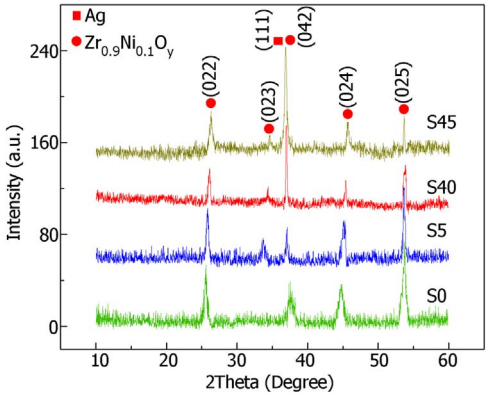

Fig. 1. XRD patterns of the Sx samples.

Table 1
The 2θ angle, d-space, Miller indices and grain size of Sx samples.

Sample	2θ ICDD standard	2θ Analyzed sample	d-spacing (Å) Analyzed sample	Size (nm)	Miller indices (*h k l*)
S0	25.982	25.98	3.42	62	(022)
	38.600	38.34	2.34	57	(042)
	44.509	44.78	2.01	43	(024)
	54.984	54.62	1.69	61	(025)
S5	25.982	26.02	3.41	61	(022)
	34.763	34.50	2.59	65	(023)
	37.934	36.9	2.43	60	(111)
	38.600	36.9	2.43	60	(042)
	44.509	45.01	2.01	42	(024)
	54.984	54.20	1.69	61	(025)
S40	25.982	26.5	3.35	60	(022)
	34.763	34.80	2.57	64	(023)
	37.934	36.8	2.43	59	(111)
	38.600	36.8	2.43	59	(042)
	44.509	45.08	2.02	41	(024)
	54.984	54.22	1.69	60	(025)
S45	25.982	26.3	3.38	58	(022)
	34.763	35.01	2.55	63	(023)
	37.934	36.7	2.44	59	(111)
	38.600	36.7	2.44	59	(042)
	44.509	45.11	2.01	39	(024)
	54.984	54.10	1.69	63	(025)

as starting compounds. Here, gold nanoparticles were used as seeds, and they were derived by reducing $HAuCl_4$ in DMF. Firstly, $HAuCl_4$ solution was prepared by mixing 10 mL of DMF with 1 mL of 0.005 M $HAuCl_4$. 170 mg of $AgNO_3$ was dissolved in DMF (10 mL) and 170 mg PVP dissolved in DMF (10 mL). A few minutes later, Ag and PVP solutions were added into $HAuCl_4$ solution with the same injection rate of 2 mL/min under vigorous stirring at 160 °C for 60 min. Silver nanoparticles began forming at this stage.

The solution was diluted with acetone and centrifuged at 2000 rpm for ~20 min. Ag nanoparticles were dispersed in Zr and Ni solution under vigorous magnetic stirring. The solution was poured into a plastic dish and sonicated for 60 min. The molar ratios of the Ag solution to $Zr_{0.9}Ni_{0.1}O_y$ solution were according to $Ag/Zr_{0.9}Ni_{0.1}O_y$=0 (named S0), 5 (named S5), 40 (named S40) and 45% (named S45).

2.3. Analyses of phase and morphology, and the permittivity and permeability measurements

The X-ray diffraction patterns of samples were recorded using X-ray diffracto-meter (model: GBC-MMA007 (2000)) with Cu-Kα (λ=1.5418 Å) radiation source. The SEM and TEM studies were carried using Scanning Electron Microscope (Model: VEGA//TESCAN-XMU) and transmission electron microscopy (Model: CM10-PHILIPS). The average grain size (grain diameter) of the samples was determined from SEM images. The theories for the permittivity and permeability measurements are "parallel plate capacitor" and "inductance" methods. The permittivity and permeability as functions of frequency were measured using test fixtures and HP 8720B analyzer. In method of capacitor, material is placed between two electrodes that form the capacitor. In method of inductance, the material is placed into a glassy toroid. The real and imaginative parts of permittivity and complex permeability were determined according to findings by Yan et al. [46].

3. Results and discussion

3.1. Structural and morphological studies of the Sx samples

Fig. 1 shows XRD diffraction pattern of various concentration of Ag doped $Zr_{0.9}Ni_{0.1}O_y$ nanocomposites. The prominent new peaks appeared at 2θ values 37.934 corresponds to silver and it is match well with the joint committee on powder diffraction standards (JCPDS) Card no. 00–001–1164. It is worth pointing out that (042) diffraction peak has overlapped with the (111) diffraction peak of Ag. Table 1 is the result of the analysis of the diffractogram of the samples with reference to the *international centre for diffraction data* (ICDD). It was also found that as the molar silver content increased, the intensity of the $Zr_{0.9}Ni_{0.1}O_y$ peaks became weaker. The four five diffraction peaks of $Zr_{0.9}Ni_{0.1}O_y$ (S45) identified with JCPDS database (01–081–0610) are typical of this Zr_3NiO phase.

The average crystallite size (D) of the different phases, evaluated by the Scherrer formula ($0.94\lambda/\beta\cos\theta$) [47] where λ=1.5408 Å and β is the high full width at half maximum (FWHM). The calculated lattice constant sizes a was 4.226 Å for Ag doped samples. The reported values for standard sample is a_O=4.079 Å (JCPDS 00–001–1164).

Fig. 2 shows the SEM photographs of $Zr_{0.9}Ni_{0.1}O_y$ and $Ag/Zr_{0.9}Ni_{0.1}O_y$ nanocomposite powders. From the SEM images, we observed that the particles are uniformly distributed. The SEM images of S0 and $Ag/Zr_{0.9}Ni_{0.1}O_y$ nanoparticle confirms the existence of relatively small crystalline nanoparticles. The particle size and distribution of nanoparticle mainly depends upon the doping concentration. The SEM images of $Ag/Zr_{0.9}Ni_{0.1}O_y$ nanoparticle reveals that the platelet like structure. When the concentration of Ag is increased, the structure of S45 becomes cluster form. It can be clearly seen that the size of the S45 nanoparticle increases with increase in molar concentration. This means with increasing the Ag in the samples, connectivity of the nanoparticle improves.

Fig. 3 demonstrates the TEM images of S45 sample nanoparticles before and after processing. It could be found that the S45 nanoparticles appeared sphere like nanoparticle with the average particle size of about 5–80 nm. A conclusion can be deduced that a much more uniform size and distribution of Ag nanoparticles rely on the cooperation of the appropriate reaction DMF and PVP [48]. Ag nanoparticles could exhibit the increase of Ag nanoparticles connectivity.

Fig. (3-b) is an image after converting to the respective binary black-white images. The black-white image corresponding to TEM image was then used to compute the filling fraction. The filling fraction of the composite is about 45%.

3.2. The permittivity and permeability analyses

The frequency dependences of permittivity for Sx composites are presented in Fig. 4. Negative ε_e' is observed in the composites with high Ag content (40, and 45 wt%), while positive ε_e' is obtained in the composite with low Ag content (5 wt%, Fig. (4-a)). Moreover, the amplitude of negative ε′ increases with increasing Ag content. Fano-